AIP | Conference Proceedings

Effect of ball-milling treatment on microstructure of in situ powder-in-tube (PIT) MgB2 tape

H. Sosiati, S. Hata, A. Matsumoto, H. Kitaguchi, and H. Kumakura

Citation: AIP Conf. Proc. **1454**, 246 (2012); doi: 10.1063/1.4730732
View online: http://dx.doi.org/10.1063/1.4730732
View Table of Contents: http://proceedings.aip.org/dbt/dbt.jsp?KEY=APCPCS&Volume=1454&Issue=1
Published by the American Institute of Physics.

Additional information on AIP Conf. Proc.

Journal Homepage: http://proceedings.aip.org/
Journal Information: http://proceedings.aip.org/about/about_the_proceedings
Top downloads: http://proceedings.aip.org/dbt/most_downloaded.jsp?KEY=APCPCS
Information for Authors: http://proceedings.aip.org/authors/information_for_authors

ADVERTISEMENT

Downloaded 25 Jun 2012 to 202.43.95.26. Redistribution subject to AIP license or copyright; see http://proceedings.aip.org/about/rights_permissions

Effect of Ball-Milling Treatment on Microstructure of *in situ* Powder-in-Tube (PIT) MgB_2 Tape

H. Sosiati[1,*], S. Hata[2], A. Matsumoto[3], H. Kitaguchi[3], and H. Kumakura[3]

[1]*Nanomaterials Research Group, LPPT, Gadjah Mada University, Yogyakarta 55281, Indonesia*
[2]*Interdisciplinary Graduate School of Engineering Sciences, Kyushu University, Fukuoka 816-8580, Japan*
[3]*National Institute for Materials Science, Tsukuba, Ibaraki 305-0047, Japan*
**hsosiati@ugm.ac.id*

Abstract In an *in situ* powder-in-tube (PIT) fabrication of MgB_2 superconducting tapes, it has been found that ball-milling treatment on a starting powder is effective for improving critical current density (J_c) of the MgB_2 tapes. In the present study, microstructures/nanostructures of MgB_2 tapes and the mechanism of the J_c enhancement by the ball milling treatment were investigated by means of scanning electron microscopy (SEM) and transmission electron microscopy (TEM) techniques. A mixed powder of Mg and amorphous B was ball milled for 4 h. The milled powder was packed in a pure Fe tube and then cold rolled into a tape specimen. A heat treatment was performed at 600°C for 1 h under an Ar atmosphere and subsequently furnace cooled. MgB_2 tape specimens without the ball-milling treatment were also prepared for comparison. A focused ion beam (FIB)-microsampling technique was used for TEM specimen preparation. The MgB_2 tape with the ball-milling treatment exhibited a dense and uniform microstructure mainly composed of nano-crystalline MgB_2. On the other hand, MgB_2 tapes without the ball-milling treatment showed inhomogeneous microstructures that comprise of a porous uncrystallized area and a crystallized one. It was also found that the averaged grain size of the nano-crystalline MgB_2 becomes smaller by the ball-milling treatment. Thus, it can be explained that the J_c enhancement by the ball-milling treatment is owing to improvements in the grain connectivity and microstructural uniformity of the crystalline MgB_2 phase in the tape.

Keywords: MgB_2, Milling, Critical current density, Transmission electron microscopy (TEM), Microstructure.
PACS: 74.70.Ad, 81.20.wk, 74.75.Sv, 68.37.Lp, 61.72,-y

INTRODUCTION

MgB_2 was discovered to be a superconductor with high critical temperature, T_c of 39 K by a Japanese research group in 2001 [1]. Research interest to improve its critical current density, J_c, has dramatically increased soon after its discovery [2-7]. High J_c property can be achieved by pinning the magnetic flux lines at impurity sites such as the crystalline imperfections that can be characterized from detailed microstructural observation.

Ball-milling treatment is one of several methods that have been proposed to improve J_c of the *in situ* PIT (powder-in-tube) MgB_2 tape. Higher-energy milling [8], particle size of starting powders Mg [9, 10] and B [11], milling media [12] and milling time [8, 13] are of important factors providing impact on J_c performance. Matsumoto *et al.* [13] have extensively investigated the improvement of J_c property by ball-milling treatment of mixed powders (Mg+B), (MgH_2+B) and (Mg+B+SiC) for various duration times. During the ball-milling process the fine boron (B) powder strongly abraded away the Mg particles, producing fresh Mg and B surfaces. This process was concluded as the main reason for Jc enhancement.

Various investigation results of ball-milled MgB_2 tapes have mostly pointed out that fine MgB_2 grain size [12], well grain connectivity [8] and uniformity [10] of crystalline MgB_2 due to ball-milling treatment are of advantage factors in improving J_c property. However, almost no effort reported on detailed microstructural change in MgB_2 tapes by ball-milling.

Presently, our attention has been devoted on the scanning and transmission electron microscopy (SEM and TEM) observations of the *in situ* PIT MgB_2 tapes to verify the microstructural differences in MgB2 tape with and without ball-milling treatment. J_c and microstructure of the ball-milled MgB_2 tape will be

International Conference on Physics and its Applications
AIP Conf. Proc. 1454, 246-250 (2012); doi: 10.1063/1.4730732
© 2012 American Institute of Physics 978-0-7354-1055-8/$30.00

Downloaded 25 Jun 2012 to 202.43.95.26. Redistribution subject to AIP license or copyright; see http://proceedings.aip.org/about/rights_permissions

discussed in comparing with that of the MgB_2 tape without the ball-milling treatment.

EXPERIMENTAL

Three kinds of *in situ* PIT MgB_2 tape specimens were used in this study. The first specimen was prepared by reducing size of the mixed powder of magnesium, Mg (325 mesh, 90%) and amorphous boron, a-B (325 mesh, 99.99%) by mechanical milling in a planetary ball mill with an Al_2O_3 vial and balls 5 mm in diameter for 4 h under Ar gas atmosphere. The second specimen was prepared by mixing the MgH_2 (325 mesh, 90%) and a-B (325 mesh, 99.99%) powders on a mortar and a pastel. Both the ball-milled and hand-milled powders were then densely packed in a pure Fe cladding, respectively. They were subsequently cold rolled into rectangular rods with the final size of about 4 mm in width and 0.5 mm in thickness and heat treated at 600°C for 1 h under a high purity Ar gas atmosphere and then furnace cooled. As a reference, the third specimen was prepared without the ball-milling treatment. The first, second and third specimens are designated as BM, W-BM and WBM-ref, respectively.

The critical current, I_c for all the specimens was measured by four-probe resistive method in magnetic fields at 4.2 K. J_c was obtained by dividing the measured I_c by the cross-sectional area of the MgB_2 core, in which the criterion of 1 μV/cm was used for I_c determination. A magnetic field was applied parallel to the tape surface.

The following analyses were carried out on the first and second specimens. The formation of MgB_2 phase and impurities was identified by x-ray diffraction (XRD) analysis. XRD specimens were prepared by mechanically removing Fe cladding from the MgB_2 core. Microstructural characterizations were performed with a SEM (FE JSM-6340F) and a TEM (FE TECNAI-F20). In this work, a focused-ion beam (FIB, HITACHI FB-2000K) microsampling (MS) technique was used for preparing TEM specimens. By this technique TEM specimen can be prepared from desired areas in the MgB2 tape and it is very useful for obtaining detail information of the microstructural characterization from the entire area of the tape correctly.

RESULTS AND DISCUSSION

J_c property

Figure 1 shows J_c for BM, W-BM and WBM-ref as a function of the magnetic field. It is obviously shown that J_c for BM at magnetic fields is higher than that of the other two. It is thought that magnetic flux pinning was enhanced by ball-milling. Despite of no ball-milling treatment applied on both W-BM and WBM-ref, J_c for W-BM is higher than that of WBM-ref. Replacing precursor Mg with MgH_2 resulted in higher crystallinity of MgB_2 and improving grain connectivity that could contribute to J_c enhancement [7]. However, the difference in J_c values between BM and W-BM would be understood from their microstructural changes resulted from the following XRD, SEM and TEM analyses.

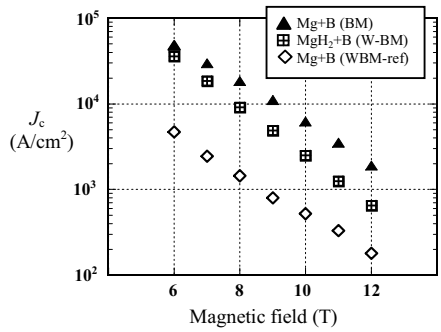

FIGURE 1. Critical current densities at 4.2 K as a function of magnetic field for the *in situ* PIT MgB_2 tapes.

XRD analysis

XRD patterns of BM and W-BM are displayed in figure 2. It can be clearly seen that the intensity of MgB_2 peaks in BM is relatively higher in comparing with that in W-BM which indicates that the volume fraction of crystalline MgB_2 phase formed in BM is higher than that of W-BM. In one hand, high volume fraction of crystalline MgB_2 phase in BM was promoted by high reactivity of milled (Mg+B) powders to form MgB_2. During the milling process, Al_2O_3 balls may strongly abrade the Mg and B powders resulting in clean surface of Mg and B [13]. On the other hand, low volume fraction of crystalline MgB_2 in W-BM is suggested due to the presence of local enrichment areas of unreacted powders. Use of MgH_2 instead of Mg explained that formation of MgB_2 phase was promoted by Mg powder with cleaner surface due to decomposition of MgH_2 before reacting with B [7].

MgO impurity is observed in both BM and W-BM in which the MgO peaks in W-BM is slightly clear than that of BM. This is possibly due to their difference in surface condition of Mg powder as mentioned above. In addition, the appearance of Fe peak in both BM and W-BM is considered as an effect

Downloaded 25 Jun 2012 to 202.43.95.26. Redistribution subject to AIP license or copyright; see http://proceedings.aip.org/about/rights_permissions

of mixing the MgB_2 core and Fe cladding during the XRD specimen preparation.

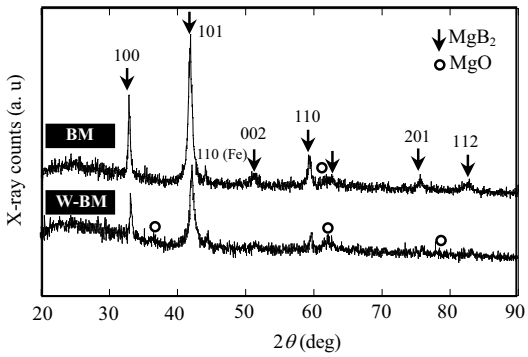

FIGURE 2. XRD patterns of the *in situ* PIT MgB_2 tapes.

SEM and TEM observations

Typical SEM micrographs of cross-sectional BM and W-BM illustrated in figure 3 (a) and (b), respectively reveal that microstructure in BM is relatively denser than that in W-BM, although micro-sized pores marked by white arrows in figure 3 (a) are observed in almost the entire area. The difference in volume fraction of micro-sized pores formed in BM and W-BM can be clearly seen in figure 3 (a) and (b). These micro defects are expected to occur during the *in situ* process. In other investigations [9, 13], however, the microstructural differences in ball-milled and without ball-milled MgB_2 in which SEM specimens were prepared by removing Fe cladding from the MgB_2 core could not be clearly distinguished. More detail microstructural differences in BM and W-BM will be shown in the following plan-view TEM images.

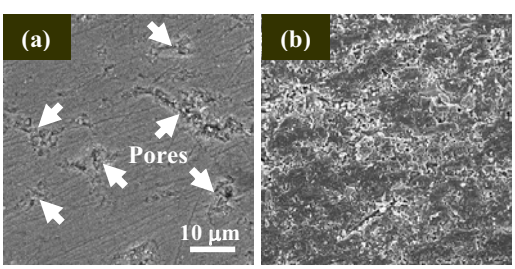

FIGURE 3. Cross-sectional SEM images of *in situ* PIT MgB_2 tapes. (a) BM and (b) W-BM.

A bright-field image (BFI), an electron diffraction pattern (EDP) and a dark-field image (DFI) of BM are demonstrated in figure 4. Microstructure in BM is characterized by homogeneous distribution of plate-like and very fine granular grains, and nano-sized pores (figure 4 (a) and (c)). An EDP in figure 4 (b) obtained from a circled area marked in figure 4 (a) shows very clear polycrystalline pattern with strong intensity of diffraction rings corresponding to the crystalline MgB_2 and MgO. A DFI in figure 4 (c) taken with a part of diffraction rings of 101_{MgB2} and 200_{MgO} reflections as indicated by a small circle in figure 4 (b) exhibits distinctly fine grain morphology of nano-crystalline MgB_2 and MgO. Owing to the very close diffraction rings of 101_{MgB2} and 200_{MgO} the presence of MgB_2 and MgO phases could not be clearly distinguished. These results suggest that reducing particle size of (Mg + B) mixed powder with ball-milling process increases the surface area of mixed powder and generates uniform contact between Mg and B powders. This would accelerate a comparatively better MgB_2 formation with heat treatment [13] resulted in dense microstructure that are mainly composed of nano-crystalline MgB_2.

Figure 5 shows typical TEM images and EDPs of W-BM. BFI in figure 5 (a) reveals microstructure feature comprising of plate-like grain structure (area

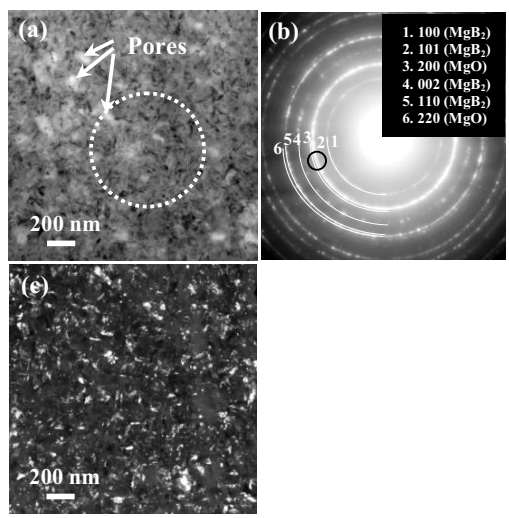

FIGURE 4. TEM images of BM. (a) BFI, (b) EDP obtained from dash-lines circle in (a) and (c) DFI obtained from small circle in (b).

`b`) and equi-axed grain structure (area `c`). EDPs obtained from area (`b`) and (`c`) are exhibited in figure 5 (b) and (c), respectively. Analyses of EDPs indicated that crystalline MgB_2 predominantly exists in plate-like grain area with small amounts of crystalline MgO as reflected from clear diffraction rings (figure 5 (b)). While an EDP in figure 5 (c) shows diffuse intensity with very weak diffraction rings attributed to the crystalline MgB_2 implying that amorphous phase has dominated the equi-axed grain area. This result confirms low volume fraction of crystalline MgB_2 in W-BM. A DFI in figure 5 (d) was taken with a part of diffraction rings of 101_{MgB2} and 200_{MgO} reflections as

Downloaded 25 Jun 2012 to 202.43.95.26. Redistribution subject to AIP license or copyright; see http://proceedings.aip.org/about/rights_permissions

indicated by a small circle area marked in figure 5 (b). This distinctly shows the morphology of plate-like and equi-axed grains, and the nano-sized pores. Inhomogeneous microstructure that comprises of crystallized area and porous uncrystallized one may be due to inhomogeneous mixed powder without ball-milling treatment and also incomplete crystallization during heat treatment. Microstructure features within the MgB2 tape as exhibited in figure 4 and 5 were not reported in other research groups [8-13].

Relationship between microstructures and J_c enhancement

As exhibited in figure 1 that J_c of the ball-milled MgB_2 tape specimen shows significant improvement under magnetic fields. It is recognizable that microstructural changes in MgB_2 tape have contributed to the J_c enhancement. Ball-milling treatment mixes magnesium and boron powders quite uniform, resulting in finer grains and fresh surface of powders. From the present SEM and TEM observations, it is clear that reducing size of starting powders by the ball milling reduce pores in the core of the tape. The reduction of pores reduces amount of oxygen during fabrication of the tape. This would result into the reduction of MgO in the ball-milled MgB_2 tape. Besides, reducing powder size and uniformity in mixed powder of magnesium and boron produce dense microstructure with high density of mainly nano-crystalline MgB_2. Although nano-pores are distributed in the entire area of the ball - milled specimen,

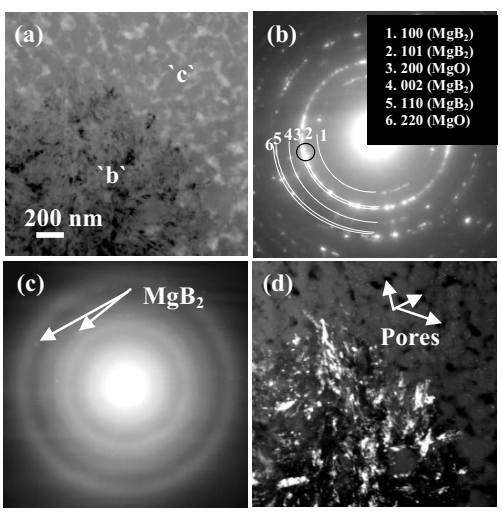

FIGURE 5. TEM images of W-BM. (a) BFI, (b and c) EDPs obtained from `b` and `c` in (a), respectively and (d) DFI obtained from small circle in (c).

uniformity of nano-crystalline MgB_2 would improve degree of grain connectivity. This is the significant factor for enhancing J_c value in BM.

In the case of the MgB_2 tape specimen without ball-milling treatment, it can be explained that degree of uniformity of starting powder is expected to be lower than that in BM specimen. It resulted in inhomogeneous microstructure as shown in figure 5. High volume fraction of amorphous-like phases and micro-pores in W-BM would decrease grain connectivity, resulting in lower J_c value than BM.

CONCLUDING REMARKS

By means of the FIB-MS technique for TEM specimen preparation of MgB_2 tapes we are successful to verify the microstructural differences in MgB_2 tape with and without ball-milling treatment. The differences in size and uniformity of the starting powder can be understood to be the cause of microstructural differences in MgB_2 tape with and without ball-milling treatment. Dense microstructure in the ball-milled MgB2 tape featured by homogeneous distribution of nano-sized plate-like crystalline MgB2 grain with high degree of grain connectivity and high volume fraction have contributed to Jc enhancement.

ACKNOWLEDGMENTS

This work was supported in part by Nanotechnology Support Project of the Ministry of Education, Culture, Sports, Science and Technology (MEXT), Japan and Research Promotion Bureau, MEXT, Japan under contract No 16-556.

REFERENCES

1. J. Nagamatsu, N. Nakagawa, T. Muranaka, Y. Zenitani and J. Akimitsu, *Nature* **410**, 63-64 (2001).
2. S. X. Dou, S. Soltanian, S. J. Horvat, X. L.Wang, S. H. Zhou, M. Ionescu, and H. K. Liu, *Appl. Phys. Lett* **81** 3419-3421 (2002).
3. S. X. Dou, W. K. Yeoh, J. Horvat, and M. Ionescu, *Appl. Phys. Lett.* **83**, 4996-4998 (2003).
4. H. Kumakura, A. Matsumoto, H. Fuji and K. Tagano, *Appl. Phys. Lett.* **79**, 2435-2437 (2001).
5. G. Grasso, A. Malagoli, C. Ferdeghini, S. Roncallo, V. Braccini, A.S. and M.R. Cimberle, *Appl. Phys. Lett.* **79**, 230-232 (2001).
6. A. Matsumoto, H. Kumakura, H. Kitaguchi and H. Hatakeyama, *Supercond. Sci. Technol.* **16**, 926-930 (2003).

Downloaded 25 Jun 2012 to 202.43.95.26. Redistribution subject to AIP license or copyright; see http://proceedings.aip.org/about/rights_permissions

7. H. Fuji, K. Tagano and H. Kumakura, *Supercond. Sci. Technol.* **15**, 1571-1576 (2002).
8. Y. F. Wu, Y. F. Lu, G. Yan, J. S. Li, Y. Feng, H. P. Tang, S. K Chen, H. L. Xu, C. S. Li and P. X. Zhang, *Supercond. Sci. Technol.* **19**, 1215-1218 (2006).
9. M. Takahashi, M. Okada, T. Nakane and H. Kumakura, *Supercond. Sci. Technol* **22**, 125017-125024 (2009).
10. H. Yamada, M. Hirakawa, H. Kitaguchi, H. Kamuakura, A. Matsumoto and H. Kitaguchi, *App. Phys. Lett*. **84**, 1728-1730 (2004).
11. Z. Ma, Y. Liu and J. Huo, *Supercond. Sci. Technol.* **22**, 125006-125011 (2009).
12. X. Xu, J. H. Kim, W. K. Yeoh, Y. Zhang and S. X. Dou, *Supercond. Sci. Technol.* **19**, L47-L50 (2006).
13. A. Matsumoto, H. Kumakura, H. Kitaguchi, H. Hatakeyama, H. Yamada and M. Hirakawa, *IEEE Trans. Appl. Supercond.* **15**, 3333-3336 (2005).

Downloaded 25 Jun 2012 to 202.43.95.26. Redistribution subject to AIP license or copyright; see http://proceedings.aip.org/about/rights_permissions